PHYSICAL REVIEW B VOLUME 55, NUMBER 18 1 MAY 1997-II

Time-dependent damage evolution and failure in materials. I. Theory

W. A. Curtin
Engineering Science & Mechanics, Materials Science & Engineering, Virginia Polytechnic Institute and State University, Blacksburg, Virginia 24061

H. Scher
Environmental Sciences and Energy Research, Weizmann Institute of Science, 76100 Rehovot, Israel
(Received 13 May 1996; revised manuscript received 6 November 1996)

Damage evolution and time-to-failure are investigated for a model material in which damage formation is a stochastic event. Specifically, the probability of failure at any site at time t is proportional to $\sigma_i(t)^\eta$, where $\sigma_i(t)$ is the local stress at site i at time t and differs from the applied stress because of the stress redistribution from prior damage. An analytic model of the damage process predicts two regimes of failure: percolationlike failure for $\eta \leqslant 2$ and ''avalanche'' failure for $\eta > 2$. In the percolationlike regime, failure occurs by gradual global accumulation of damage culminating in a connected cluster which spans the system. In the avalanche regime, failure occurs by rapid growth of a single crack after a transient period during which the critical crack developed. The scalings of the transient period, the subsequent crack dynamics, and the time-dependent probability distribution for failure are determined analytically as functions of the system size and the exponent η. Specific predictions are that failure is more abrupt with increasing η, failure times scale inversely with a power of the logarithm of system size, and the distribution of failure times is a double exponential and broadens with increasing η, so that the failure becomes less predictable as it is becoming more abrupt. The conditions for the transition to the rapid growth regime are identified, offering the possibility of early detection of impending failure. In a companion paper, numerical simulations of this failure process in two-dimensional lattices are compared in detail to the analytical predictions. [S0163-1829(97)04117-9]

I. INTRODUCTION AND PROBLEM STATEMENT

Failure under load is a major limitation to the application of many materials, especially structural materials at elevated temperatures. Understanding the mechanisms by which damage forms, coalesces, and leads to failure, and the associated time scales for these phenomena, is a critical area of research for engineering applications of structural components. These time-dependent failure phenomena are also often nonlinear in both time and stress, making the development of predictive models of damage accumulation and failure particularly challenging. Models are necessary, however, for several reasons. First, it is costly and time consuming to perform enough experiments in the laboratory to fully identify the (unknown) probability distribution of any failure process, which is necessary to establish material or component reliability. Second, the failure in many materials can be driven by weak-link considerations, i.e., the material fails upon the first occurrence of a critical amount of damage anywhere in the material. This leads to a natural dependence of failure time and/or strength on material volume, and to a scaling of the associated probability distributions with material volume. Knowledge of the expected analytic behavior of such distributions under various degradation modes can then guide the fitting of experimental data and the extrapolation of such data to either (i) much larger system sizes than can be tested in controlled experiments, such as full-scale components, or (ii) much longer life situations, usually at lower stresses, than can be tested in acceptable laboratory time scales. Third, the development of predictive models can help identify precursors to failure and rank the severity of damage, so that appropriate nondestructive evaluation techniques might identify precursor damage prior to failure. The expected remaining life of the material might then be accurately estimated or the component removed from service prior to catastrophic failure.

Stress-driven damage accumulation is particularly important in brittle materials such as ceramics at high temperatures, because the critical amount of damage required to cause failure can be rather limited and difficult to detect. Several different types of mechanisms can operate in determining damage growth in such materials. The clearest damage mechanism is the slow growth of preexisting cracks due to chemical attack at the crack tips.[1] The existing cracks grow at rates determined by the kinetic breaking of bonds, which is usually associated with the applied stress intensity at the tips of the cracks. Larger cracks grow faster, and the largest crack is the first to reach a critical stage at which rapid, unassisted crack growth can occur. This situation is thus easily described with knowledge of the underlying initial flaw population and the kinetics of the crack growth. Crack interactions are usually negligible because the population is dilute, and hence the single-crack problem combined with a growth law is sufficient for adequate representation of the failure behavior.[2] Less well defined is failure by ''creep damage,'' which is damage that does not evolve from the preexisting flaws but rather develops due to time-dependent deformation under load which causes nucleation of voids/cavities/cracks. Such damage generally controls failure at low applied stresses where preexisting flaws are blunted and do not extend.[3] This implies that the failure times for such processes are also much longer, making testing and assess-

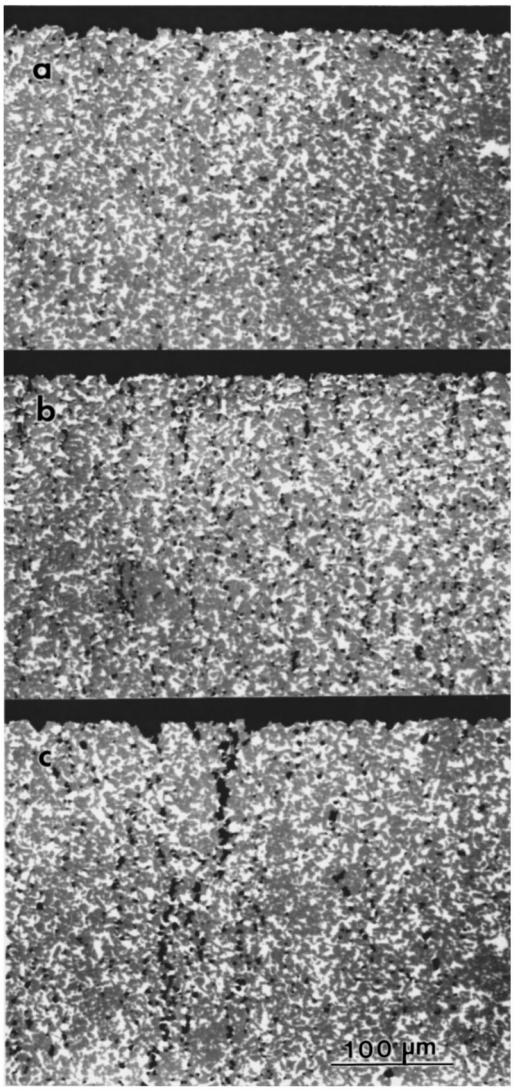

FIG. 1. Evolution of cavity damage in siliconized SiC (Carborundum Company KX-01) under flexure testing at 1300 °C. Note the formation of extended cavity clusters perpendicular to the applied tensile load (applied stress is horizontal). Figure obtained from Dr. S. Wiederhorn [J. Am. Ceram. Soc. **79**, 977 (1996)].

ment difficult. Since the damage is not related to the initial flaw distribution, the statistical distribution of evolving damage is not clearly determined. Similar to the slow crack growth mechanism, the damage nucleation and growth can be very sensitive to stress state. Then, damage localization occurs because local damage enhances the stresses in its neighborhood and drives further local damage faster than at points remote from the damage.

Detailed models for the basic dynamics of damage evolution under such ''creep'' mechanisms are not well developed. Models such as the semiempirical Coleman model for the statistical distribution of time-dependent fiber strengths are often used but do not accommodate specific damage mechanisms.[4] A common empirical estimate is the Monkman-Grant approach, which connects creep rate to failure time by postulating a relationship between the minimum (steady-rate) creep rate $\dot{\varepsilon}_{\min}$ and failure time t_f of the form $\dot{\varepsilon}_{\min}^{m} t_f = C$, where C is some constant and m is a parameter.[5] The Monkman-Grant approach implicitly connects creep and

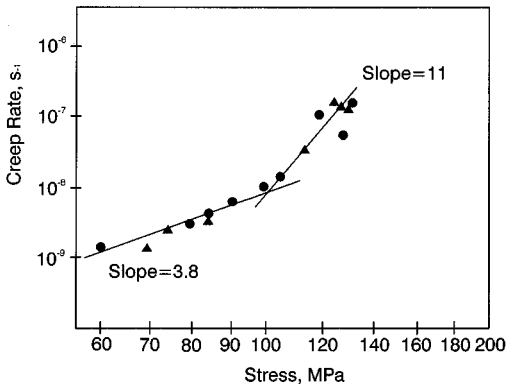

FIG. 2. Creep strain rate versus stress for siliconized SiC, indicating high stress exponent ($\eta \approx 11$) for stresses above 140 MPa where cavitation is observed.

failure, and in essence assumes that failure occurs at some critical creep strain, which might be independent of actual applied stress if $m=1$. Underlying models which generate such relationships from some microstructural damage evolution law do not exist, to our knowledge.

Our goal here is to examine damage evolution and failure within the framework of one well-defined damage formation law. We focus on capturing the major dynamics of the damage evolution, induced strain, and ultimate material failure, and their dependences on system volume and nonlinearity in the stress dependence of the damage evolution in systems for which the ''damage'' is a probabilistic, nucleated event driven by local stress. One material which appears to behave in this manner is the composite Si/SiC.[6–8] Under load at elevated temperatures, cavities form in this material between SiC/SiC grain-boundary facets, as shown in Fig. 1. The cavities extend across the entire grain boundary and the rate of cavitation is strongly dependent on the level of applied stress ($\propto \sigma^{11}$) above a threshold strain of 100 MPa (Fig. 2). Furthermore, the spatial distribution of cavities is not random; clustering occurs in the form of arrays of cavities in planes roughly perpendicular to the tensile load axis (Fig. 1). Sensitivity of the cavitation rate to *local* stress is suggested by the clustering behavior and verified by the observations that cavitation occurs preferentially in the large tensile stress field ahead of intentionally introduced indent cracks under small remote loads. The cavity arrays are not formed by the slow crack growth mechanism because the cavities are physically disconnected, being separated by uncavitated boundaries or, more often, pools of very ductile silicon. The cavities are responsible for most of the creep deformation in the material, lead to strength degradation by cavity coalescence in time, and ultimately some cavities coalesce to form a sufficiently large cavity that drives macroscopic failure. The failure time decreases with increasing applied stress, and over a range of temperatures and loads the failure and creep data can be fit to a Monkman-Grant relationship with an unusual exponent of $m=1.45$.[6] The progression of damage in time and the dependence of failure time on microscopic aspects of the damage formation are general features occurring in many other materials and motivate the study of general damage models to predict the remaining strength and reliability in such materials.

In developing a model which is general but relevant to

materials such as Si/SiC, we first recognize several key features of the deformation and damage. First, the presence of fully extended facet-sized cavities suggests that cavity formation is controlled by a critical nucleation step, and is thus a probabilistic event. Second, the sensitivity of cavitation rate to stress and the observation of cavity clustering both suggest that this cavitation rate is dependent on the *local* stress acting across each grain boundary at any given time. We thus consider an elastic material consisting of an ordered array of connected, cavitatable sites. At each site i, the local (tensile) stress $\sigma_i(t)$ consists of the applied load plus additional loads transferred to site i due to previous cavitation damage at other sites. The cavitation rate $r_i(t)$ (probability of cavitation per unit time) is assumed to have power-law dependence on the local tensile stress:

$$r_i(t) = A\sigma_i(t)^{\eta}. \tag{1}$$

Here, A is a rate prefactor and the exponent η determines the sensitivity of the cavitation rate to applied stress; both can be dependent on temperature. A power-law rate is used because it generates a power-law dependence of strain rate on applied stress, as observed in Si/SiC.[6–8] The form of Eq. (1) is also similar to that often assumed for the stress dependence of slow-crack growth, although a different physical mechanism is envisioned.

The evolution of damage in an array of sites obeying Eq. (1) is complex. Initially, the material is undamaged and all sites oriented perpendicular to the applied field have the same cavitation. Isolated cavities are then nucleated randomly throughout the material. Stress redistribution around the existing cavities increases the stress at nearby sites in the plane perpendicular to the applied load. The enhanced stress preferentially drives cavitation at sites near to the existing cavities, but initially there are many more sites remote from the existing cavities that are subject to essentially the applied stress. The location of subsequent cavities must be determined probabilistically, and each site i has a relative rate given by $r_i(t)/\Sigma_j r_j(t)$. The typical time Δt required to form the next cavity is simply the inverse of the sum of the rates, $\Delta t = 1/\Sigma_j r_j(t)$. As time proceeds, new cavities form, cavity clusters form, and the stress at the tips of larger cavity clusters is generally larger than that at smaller clusters. This stress enhancement continues to drive the formation of larger clusters faster than smaller clusters, but is mitigated against by the greater number of smaller clusters and/or uncavitated sites. Cavitation continues until failure, at which point one cavity cluster spans the entire length of the system—no explicit condition for the onset of actual ''fast-fracture'' crack growth is considered. The damage evolution is thus controlled simultaneously by the current spatial distribution of clusters and the enhanced rates prevailing around these clusters.

For the above model, the special case of $\eta = 0$ corresponds to the random-dilution percolation problem. The local stress does not affect the cavitation rates: all rates are always equally likely. Damage forms randomly throughout the material until a connected percolation cluster is formed after a critical volume fraction p_c of sites are damaged. For the cases where $\eta > 0$, there is some enhancement of the rates due to enhanced local stresses and hence some tendency toward damage localization. The major issue addressed here is how such effects are manifest in the damage evolution and failure of the material. Some preliminary work toward this goal has been published previously.[9]

To go from a qualitative understanding of the consequences of Eq. (1) in tandem with some load transfer rules to a quantitative calculation of the damage accumulation and actual failure point is a daunting task. The myriad of damage cluster shapes (especially for two and three dimensions), long-range elastic load transfers, and cluster interactions that are possible makes exact analytic calculations hopeless. Numerical simulations can include many of the necessary specific details, and will be discussed at length in the companion paper. Previous simulation work by Hansen, Roux, and Hinrichsen has, however, uncovered some fascinating results regarding the failure as a function of size and the parameter η. Hansen, Roux, and Hinrichsen studied the accumulated damage at failure in simulation studies of electrical fuse networks which exhibit many features identical to elastic networks.[10] For $\eta \leqslant 2$, a linear dependence of total damage on system size, $N_f \propto N_T$, was found. However, for $\eta > 2$ Hansen, Roux, and Hinrichsen found a sublinear dependence, $N_f \propto N_T^{\gamma}$ with $\gamma < 1$ and γ decreasing with increasing η. The fixed damage fraction N_f/N_T for small η is as found in the limit $\eta = 0$, and furthermore the fluctuations in failure damage around the mean were found to be similar to those obtained in the percolation problem. The decreasing damage fraction at higher η was accompanied by an associated failure mode dominated by one large crack. These results suggest that the two regimes of η correspond to intrinsically different modes of failure, ''percolationlike'' and ''avalanchelike.'' Simulations can provide guidance, but it is difficult to extend simulations to realistic component size scales and to generalize the results to other load transfer rules. An approximate analytic formulation capable of capturing the major dynamics and scaling is clearly necessary, and is the subject of this paper.

Theoretical work on time-dependent damage evolution and failure for the damage nucleation problem described by Eq. (1) has been performed by several workers. Most notably, Phoenix, Tierney, and Kuo have considered this problem in two dimensions under the restriction that the damage clusters are linear and that all of the stress from a cluster of cavities is transferred to the immediate neighboring sites at the cluster ends.[11–14] They primarily investigated the asymptotic limits of the model, i.e., the regime of large η and short times (low failure probabilities), and uncovered interesting features of the failure. Our work makes similar assumptions at the outset and, although approached quite differently, shows very similar features to those of Tierney and co-workers and in some ways validates their asymptotic results for much smaller values of η. We will discuss their results in more detail at the end of this paper.

The remainder of this paper is organized as follows. In Sec. II we present an analytical model for the damage evolution and failure under the local damage process described by Eq. (1). We then demonstrate the existence of two regimes of failure within the model as observed in simulations. In Sec. III, we derive analytic expressions for the failure time, its scaling with system size, and the precursor conditions prior to failure, as functions of the driving parameters. In Sec. IV we present results for the failure time distribution, and its size-scaling behavior. Section V contains further dis-

cussion. In the Appendix, we discuss the inclusion of mean-field interactions into the model. A companion paper describes extensive numerical simulations and comparisons with the analytic results described in this paper.

II. ANALYTIC MODEL FOR DAMAGE AND FAILURE

A. Damage accumulation and macroscopic observables

Our model material consists of N_T interconnected, damage-prone boundaries, with each boundary having z neighbors. As the damage evolves, each boundary is either uncavitated or part of a cluster of cavities of size $c \geqslant 1$. The damage state at any instant can thus be characterized by the distribution of cavity clusters $N(c,t)$, where $N(c,t)$ is the number of clusters of size c in the material at time t, and their spatial locations. In principle, the time evolution of $N(c,t)$ depends on the complicated stress fields generated by the presence of cavity clusters throughout the material, and a particular size c does not specify a precise geometry of the cluster. We posit that, because the stresses at the tips of a cluster perpendicular to the loading axis experience the highest stresses, that the cluster geometry is preferentially quasilinear and oriented mainly perpendicular to the loading axis. Then, the size c refers to the length of well-defined cluster in two dimensions (2D), and is related to the cluster area in 3D problems. Before discussing means of calculating $N(c,t)$, it is constructive to assume that (i) $N(c,t)$ has been supplied by some means and (ii) the cavity clusters do not interact substantially so that cavity cluster correlations can be neglected, and then to demonstrate how essentially all of the time-dependent macroscopic properties of the material can be calculated. This is done below.

The time-dependent strain in the material is composed of two parts. The first part is the elastic strain arising from a damage-reduced Young's modulus $E(t)$,

$$\varepsilon_{\rm el} = \sigma_{\rm app}/E(t). \tag{2}$$

$E(t)$ can be related to the cavity cluster distribution using a mean-field theory[15] as

$$E(t) = E(0)\left[1 - \frac{\beta}{N_T}\sum_{c \geqslant 1} c^d N(c,t)\right] \tag{3}$$

for planar cracks in d dimensions, with β a parameter ($\beta = 0.47\pi$ for a continuum elastic medium in 2D).[16] The second contribution is the strain due to the creation of new volume V_c upon each cavity formation, as discussed by Raj,[17] and is

$$\varepsilon_{\rm vol} = \frac{1}{3}\frac{V_c}{L_{11}}\sum_{c \geqslant 1} cN(c,t), \tag{4}$$

where L_{11} is the length of the specimen along the tensile axis. Both contributions to the strain are determined by $N(c,t)$.

The total number of clusters of size equal to, or greater than, c is a useful quantity for various reasons, as we shall see. Normalizing this cumulant by the total number of sites, or material volume, then yields the generalized ''risk of rupture'' function

$$R(c,t) = \sum_{c' \geqslant c} N(c',t)/N_T. \tag{5}$$

The failure probability due to clusters of size c or larger (i.e., the probability of appearance of a cluster $\geqslant c$) at time t is obtained using standard weak-link arguments as

$$P(c,t) = 1 - e^{-N_T R(c,t)}. \tag{6}$$

The typical (63.2% level) largest cluster c^* at time t then satisfies

$$N_T R(c^*,t) = \sum_{c \geqslant c^*} N(c^*,t) = 1, \tag{7}$$

i.e., there is typically one cluster at least as large as size c^* in the system.

The characteristic failure time t_f is the time at which the typical largest crack size c^* is equal to the transverse sample length L, $c^* = L$. Mathematically, failure is expressed by

$$N_T R(L,t_f) = 1. \tag{8}$$

Since it does not make sense to talk about cracks larger than L, we must have $R(L,t) = N(L,t)/N_T$ and hence failure occurs at a mean time t_f satisfying $N(L,t_f) = 1$. The probability of failure is then $P(L,t)$, with P given in Eq. (6).

It is possible that fast crack propagation emanating from the largest cluster can interrupt the nucleated damage process and cause failure. In such a case, most of the material lifetime is taken up in the initial formation, via cavitation, of the critical defect size $c_{\rm crit}$ needed for crack propagation, and so the failure time satisfies $N_T R(c_{\rm crit},t_f) = 1$ and the probability of rupture is $P(c_{\rm crit},t)$ following from Eq. (6). The critical size can be obtained from fracture mechanics consideration of the time-dependent tensile strength, i.e., the strength of the material after surviving a certain time at some applied load. A strength S is obtained from a defect of size $c = (YK_{ic}/S)^2$, with Y a geometrical parameter and K_{ic} the material toughness at the test temperature. Hence, the characteristic time-dependent strength is

$$S(t) = \frac{K_{ic}}{Yc^{*1/2}}. \tag{9}$$

As time progresses c^* increases and the strength decreases. Failure during the creep process occurs at a size $c_{\rm crit}$ satisfying Eq. (9) with S equal to the applied stress. Here, we will be interested in the largest cluster size versus time, but will not consider further the issue of failure by fracture from the largest cluster.

Equations (2)–(9) provide the mathematical basis for calculating essentially all of the quantities of interest during the creep damage process from the underlying cluster distribution $N(c,t)$. As yet, we do not know $N(c,t)$ and we turn to that formidable problem below.

B. Analytic model of damage evolution

To make analytic progress on understanding the subtle aspects uncovered by numerical simulations, and the experimental results on materials such as Si/SiC, requires an ap-

proximate analysis which retains the key physics. We start by rescaling the underlying rate law by factoring out the applied stress,

$$r_i(t) = A\sigma_{\rm app}^{\eta}(\sigma_i/\sigma_{\rm app})^{\eta}. \tag{10}$$

In this form, we can identify an underlying rate $r_0 = A\sigma_{\rm app}^{\eta}$ or time scale $\tau_0 = r_0^{-1}$, and a dimensionless rate enhancement factor $(\sigma_i/\sigma_{\rm app})^{\eta}$ describing how the local stress at i modifies the nucleation rate at i relative to the reference rate r_0. We then recognize that for evolving damage, the damage rate is highest at the tips (perimeter) of existing damage where the local stress transfer is highest. We therefore focus attention on these tip sites by assuming that all sites in the system are either (i) tip sites, at the tip of a cluster of size c units and under an enhanced stress denoted σ_c, (ii) damaged sites in the cavity clusters themselves, which are under no stress, and (iii) all remaining nontip, nondamaged sites, under only the applied stress $\sigma_{\rm app}$. This division of sites into three categories eliminates long-range interactions between existing damage and linking together of two existing clusters, issues we will address later. Then, the quantity to determine is the cluster size distribution $N(c,t)$ which is the number of size c clusters at time t. Within the assumptions above, size c clusters can only form via the growth of size $c-1$ clusters and can only be lost by growth to size $c+1$ clusters. Hence, the evolution of $N(c,t)$ follows a Master Equation:

$$\frac{dN(c,t)}{dt} = zA\sigma_{c-1}^{\eta}N(c-1,t) - zA\sigma_c^{\eta}N(c,t) \quad c \geqslant 1, \tag{11}$$

where the growth rate of a size c cluster is $zA\sigma_c^{\eta}$ with z being the number of possible growth sites at the tips of the cluster (e.g., $z=2$ for a $1-d$ line, $z=4$ for the triangular lattice) and $\sigma_0 = \sigma_{\rm app}$. $N(0,t)$ is the number of ''size 0'' cavities, or nondamaged/nontip sites and satisfies the sum rule

$$N(0,t) = N_T - \sum_{c \geqslant 1} (c+z)N(c,t). \tag{12}$$

Defining a dimensionless time $\tau = t/\tau_0 = tA\sigma_{\rm app}^{\eta}$ and recognizing that the stress enhancement is generally proportional to the applied field $\sigma_c = K_c\sigma_{\rm app}$, where K_c is the stress concentration factor at each of the z tip sites of a size c cluster, allows us to rewrite Eq. (12) in the nondimensional form

$$\frac{dN(c,\tau)}{d\tau} = \alpha_{c-1}N(c-1,\tau) - \alpha_c N(c,\tau), \tag{13}$$

where $\alpha_c = zK_c^{\eta}$ is the dimensionless growth rate and $\alpha_0 = 1$. Equation (13) contains all of the damage evolution dynamics that are considered in the present model, and is a well-defined set of coupled equations for $N(c,\tau)$ in terms of the underlying parameters K_c and η, and the total number of sites N_T entering into the initial conditions. Equation (13) was proposed earlier in Refs. 9 and 18.

The solutions to the coupled set of equations for $N(c,\tau)$ can be obtained analytically by using Laplace transforms and by approximating $N(0,t) = N_T$.[18] Of particular interest are two limiting cases, corresponding to short and long times for any crack size c.

In the limit $\alpha_c\tau/c \ll 1$ the solution to Eq. (13) is obtained by neglecting the $-\alpha_c N(c,t)$ ''depletion'' term on the right-hand side (rhs) of Eq. (13), leading to

$$N(c,\tau) = \left(\prod_{c'=1}^{c-1} \frac{\alpha_{c'}}{c'} \right) \tau^c. \tag{14}$$

In this regime, $N(c,\tau)$ is rapidly decreasing for increasing cluster sizes c at any fixed time $\tau < 1$. If the ratio α_c/c is not an increasing function of c, then Eq. (14) is the solution for $N(c,t)$ for all times $\tau < 1/\alpha_1$ and the cluster size distribution decreases at least exponentially fast with increasing cluster size, i.e.,

$$N(c,\tau) \leqslant N_T e^{c(\ln\tau)}. \tag{15}$$

Large clusters are thus very unlikely; most of the accumulated damage is tied up in smaller clusters. From Eq. (5), we also have a risk of rupture function $R(c,\tau)$ that decreases at least exponentially fast.

In the long-time limit $\alpha_c\tau/c \gg 1$ the solution to Eq. (13) becomes simply[18]

$$N(c,\tau) \propto N_T\alpha_c^{-1}, \tag{16}$$

which can partially be motivated by considering the ''steady-state'' condition $dN(c,\tau)/d\tau = 0$ of Eqs. (13). In this regime, the associated largest cluster size c^* defined by Eq. (7) can be rewritten by taking the derivative of $R(c,t)$ in Eq. (5), substituting Eqs. (13) for the $dN(c,t)/dt$ terms, performing the summation, integrating, and considering $c = c^*$. This yields

$$\int_0^{\tau} d\tau' \, \alpha_{c^*-1}N(c^*-1,\tau') = 1, \tag{17}$$

which states that the integrated flux of clusters growing into size c^* equals unity. Hence, as the largest cluster enters the long-time regime of Eq. (16) then c^* must increase rapidly with time to satisfy Eq. (17). This rapid growth is the avalanche observed in the simulations and always occurs if the long-time regime can be reached prior to failure. This can only occur if α_c/c is an increasing function of c.

III. PREDICTIONS OF FAILURE BEHAVIOR

We now apply the model to understand the fundamentally different failure behaviors for $\eta \leqslant 2$ and $\eta > 2$ observed in the simulation study by Hansen, Roux, and Hinrichsen.[10] In these simulations, the stress concentration factors scale essentially as the square root of cluster size, and so we assume the form $K_c = (1 + 1/z)c^{1/2}$. This form distributes the stress of a size 1 cavity equally to the z neighbors at its tips, and for larger clusters the desired square-root dependence for linear systems obtains.

A. Percolationlike failure: $\eta \leqslant 2$

For $\eta \leqslant 2$, the short-time limit $\alpha_c\tau/c < 1$ applies to *all* cluster sizes for times $\tau < 1/\alpha_1$ because α_c/c is not increasing with c. Damage occurs as a gradual proliferation of small clusters which ultimately do link together to form a large

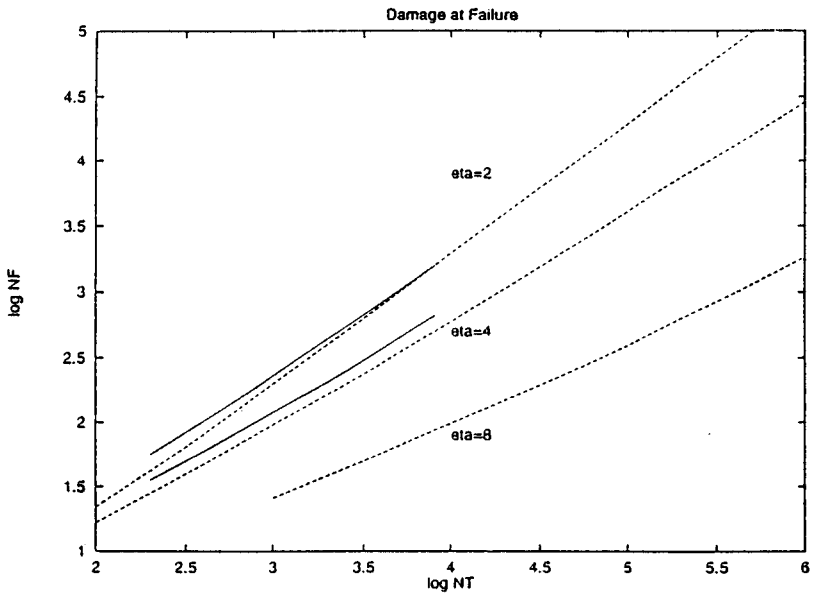

FIG. 3. Predicted damage at failure N_f versus system size N_T for various η. Solid lines are simulations on electrical fuse networks (Ref. 10); dashed lines are predictions of present model.

crack. Such linking processes are *not* contained in our model. But, they only occur late in life just as in the percolation problem ($\eta=0$), where it is observed that the divergence of the correlation length and largest cluster size are narrowly confined to a region near the critical point. Because no single large cracks grow on their own, it is reasonable to estimate the failure time as the point at which the elastic modulus of the highly damaged system has decreased to zero, $E(\tau_f)=0$. This is a mean-field estimate for the ''critical'' percolation point and therefore is expected to capture the general behavior but not give a highly accurate value for the failure or total damage $p_c=N_f/N_T$ at failure.

To determine the failure time τ_f, we first assume the short-time solution to be accurate up to τ_f, i.e., assume that $\tau_f<1/\alpha_1$. We can then substitute the short-time solution for $N(c,\tau)$ [Eq. (14)] into the mean-field expression for the elastic modulus [Eq. (3)], set the elastic modulus to zero, and solve for the required time τ_f. The case of $\eta=2$, which is the largest value of η for which the short-time solution holds for times shorter than $1/\alpha_1$, yields an analytic result. For $\eta=2$, Eq. (14) reduces to $N(c,t)=N_T\alpha_1^{c-1}\tau^c$, where $\alpha_1=z(1+1/z)^2$. Subbing into Eq. (3) and setting $E=0$ leads to a failure time τ_f satisfying

$$\frac{\alpha_1}{\beta}=\sum_{c=1}^{\infty} c^2(\alpha_1\tau_f)^c. \tag{18a}$$

After performing the sum and rearranging, the failure time is the solution of a quadratic equation which we choose to write as

$$\frac{\alpha_1\tau_f}{(1-\alpha_1\tau_f)^2}=\frac{z(1+1/z)^2}{\beta}. \tag{18b}$$

Equation (18b) always has a solution satisfying $\alpha_1\tau_f<1$ for any value of the coefficient β appearing in the mean-field elastic modulus expression. For $\eta<2$, a similar conclusion holds but the result cannot be expressed in a simple analytic form. Since failure does occur within the range of validity of the short-time solution, the use of the short-time solution is thus validated *a posteriori*.

For $\eta\leqslant 2$ the failure is thus percolationlike, even though there is some tendency of the stress-dependent damage term to drive preferential large cluster development. Up to the power of $\eta=2$, the rate enhancement by stress concentrations is not strong enough to compete against the more frequent ''random'' evolution of many smaller clusters growing at lower rates. The small-cluster damage dominates the total damage and leads to global percolationlike failure before enough time has elapsed for any large self-propagating clusters to emerge (i.e., failure occurs before $1/\alpha_1$). A single large cluster does exist at failure, but has been formed by the fairly rapid coalescence of smaller clusters just as the critical point is being reached.

For $\eta\leqslant 2$, the failure time is also predicted to be independent of the system size N_T, and the total damage at failure scales linearly with the system size, in agreement with the simulations.[10] Numerical solutions of Eq. (13) with the mean-field failure condition $E(\tau_f)=0$ yield predictions for the total damage at failure versus system size and η as shown in Fig. 3. The quantitative agreement with the simulation results for $\eta=2$ is quite good, indicating the general accuracy of the mean-field estimate of the failure point with no adjustable parameters.[9]

B. Avalanche failure: $\eta>2$

For $\eta>2$, the short-time limit is always exceeded for some larger cluster sizes prior to global failure. Under such conditions, the cluster size distribution is no longer exponentially decreasing but has a large-c tail which decays slower than exponentially. From Eq. (17) it is clear that the largest cluster c^* can reach a stage at which it grows rapidly across the material to cause failure. Numerical solutions of the full system of Eq. (13) for the largest cluster c^* versus time τ are shown in Fig. 4 for $\eta=4$ at two system sizes; the fairly

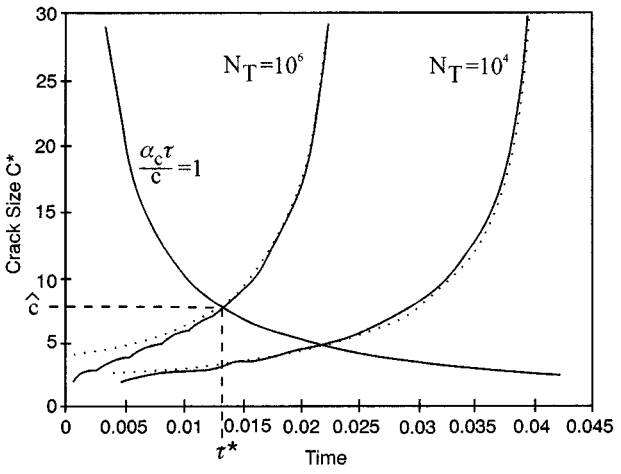

FIG. 4. Growth of typical largest cluster c^* versus time, for $\eta=4$ and $N_T=10^4$, 10^6. The solid lines are full numerical result; dashed lines are the approximate result. Also shown is demarcation line for short-time/long-time crossover, determined by $\alpha_c \tau/c=1$.

sudden, rapid growth of the largest crack after some transient period and the size dependence of the phenomenon, are clearly exhibited in these results. Predictions for the total damage N_f at failure versus η and system size N_T are shown in Fig. 3, and again there is good quantitative agreement with the simulations with essentially no adjustable parameters in the theory.[9]

During the rapid-growth period exhibited in Fig. 4, smaller clusters can continue to grow but they are not necessary to complete the failure. For increasing system sizes N_T the onset of rapid growth occurs at earlier times, and so there is less other damage and interactions of the largest cluster with the smaller clusters can be neglected for large system sizes.

IV. FAILURE TIME SCALING IN THE AVALANCHE REGIME

A. Scaling of the mean

In the percolation regime $\eta \leqslant 2$, there is no size dependence of the mean failure time or damage at failure. Nor is the size dependence in the avalanche regime $\eta > 2$ evident from the form of Eqs. (13) or (17), although it is apparent in Figs. 3 and 4. The evolution of modulus, strain, and failure time distribution can be calculated directly from Eq. (13) and then Eqs. (3)–(7), but this does not provide any physical insight into the factors and events which actually control the time-to-failure and its distribution versus size N_T and η. Nor does it provide guidance for any observed scaling behavior. In addition, one would like to identify any signature of incipient failure so as to anticipate failure in any one sample, and one would like such a signature to have the same size and η dependence as the failure time itself. Thus it is necessary to analyze the predicted damage evolution more carefully to clearly extract the origin of the size scalings.

In the avalanche regime ($\eta > 2$), one single large ''crack'' ultimately controls the failure and so we focus on the typical largest cluster, denoted previously as c^*. The nature of the long-time solution Eq. (16) to Eq. (13) stems from the fact that when a crack reaches a sufficient size (as yet unknown) it tends to propagate without any ''supply'' from smaller crack sizes. We apply this notion to the typical largest c^* crack that ultimately causes failure. We would like to determine the time, denoted τ^*, at which the largest crack c^* emerges from the distribution of smaller cracks and starts the avalanche process. We show below that establishing the time τ^* then leads to a determination of the size scaling of both the failure time τ_f and its distribution. Two key steps enable us to identify τ^* and obtain a relationship between τ^* and τ_f: (1) a simplified analytic solution for the largest crack $c^*(t)$ as a function of time in the avalanche regime, and (2) the criterion that τ^* is the time at which the largest crack emerges from the small-crack/short-time solution for $N(c,t)$.

To follow the evolution of the largest crack, we take the definition of $c^*(t)$ from Eq. (7) and differentiate with respect to time to obtain

$$-\frac{dc^*}{d\tau} N(c^*,\tau) + \sum_{c=c^*}^{\infty} \frac{dN(c,\tau)}{d\tau} = 0. \tag{19}$$

The sum can be rewritten, using Eq. (13), to give

$$\frac{dc^*}{d\tau} = \alpha_{c^*} \left(\frac{\alpha_{c^*-1} N(c^*-1,\tau)}{\alpha_{c^*} N(c^*,\tau)} \right), \tag{20}$$

where the rhs has been multiplied and divided by α_c^*. Strictly in the avalanche regime, we can then use the long-time solution of Eq. (16) to obtain

$$\frac{dc^*}{d\tau} = \alpha_c^* . \tag{21}$$

The driving equation is that for a single crack growing at a rate proportional to its size. This demonstrates that the largest crack in the avalanche regime does grow independently of the supply of smaller cracks. The evolution of Eq. (21) can now be integrated starting from a size c at some time τ and ending at the known final value of $c^*=L$ at the failure time τ_f. For the case of square-root stress-enhancements [$\alpha_c = z(1+1/z)^{\eta} c^{\eta/2}$], one obtains the result

$$c^*(\tau) = L \left(1 + \frac{z(1+1/z)^{\eta} (\eta/2-1)(\tau_f - \tau)}{L^{1-\eta/2}} \right)^{1/1-\eta/2} . \tag{22}$$

This expression for the largest crack c^* versus time is compared to the full solutions, obtained from Eqs. (13) and (7), in Fig. 4 for the case of $\eta=4$ and $N_T=10^4,10^6$. In Fig. 4, the $c^*-\tau$ plane is divided by the line $\alpha_c^* \tau/c^*=1$ corresponding to the two regimes of short times/small cracks and long times/large cracks. Equation (22) is an excellent approximation to the exact result in the entire $\alpha_c^* \tau/c^* > 1$ (the upper right in the Fig. 4). As discussed above, c^* must be in this regime for the avalanche to occur; if c^* is in the short-time regime then self-sustaining growth cannot occur. The time at which $c^*(\tau)$ crosses into the long-time/large-crack regime is postulated here to be the avalanche onset time τ^*, and is obtained from the simultaneous solution of Eq. (22) and the condition

$$\alpha_c^* \tau/c^* = 1. \tag{23}$$

The result is

$$\tau^* = (1-2/\eta)\,\tau_f + \frac{2}{\eta z(1+1/z)^{\eta} L^{\eta/2-1}}, \tag{24}$$

with the second term being vanishingly small for large system sizes. The associated critical cluster size at this point is denoted $\hat{c} = c^*(\tau^*)$. This result is equivalent to assuming that as soon as the largest crack reaches the size $\hat{c}$, it leaves the short-time regime and grows forward to failure, according to Eq. (22), in a time $\tau_f - \tau^*$. *The large L limit of Eq. (24) also implies that the size scaling of the real failure time τ_f is then identical to that of the onset time τ^*. This is a main result of this paper.*

The relationship between τ^* and τ_f is interesting, but we do not have any expression for either of the two independently. A major advantage of working with the τ^* identified here is that, being on the border of the short-time regime, we can use the analytic short-time solutions for $N(c,\tau)$. We obtain the scaling of τ^* with system size by using the short-time solution Eq. (14) for $N(c,\tau)$, setting $N(\hat{c},\tau^*)=1$, and solving this simultaneously with Eq. (23) ($\alpha_{\hat{c}}\tau^*/\hat{c}=1$) yields, using Stirling's approximation along the way, the critical cluster size

$$\hat{c} = \frac{\ln(N_T)}{\eta/2-1} - \frac{\ln(z(1+1/z)\,\eta)}{\eta/2-1} + \ln(\sqrt{2\pi}) - \frac{1}{2}\,\frac{\eta/2+1}{\eta/2-1}\,\ln(\hat{c}), \tag{25}$$

where the size scaling is essentially controlled by the first term. The associated onset time τ^* then simply

$$\tau^* = \frac{\hat{c}}{\alpha_{\hat{c}}} \propto [\ln(N_t)]^{1-\eta/2}, \tag{26}$$

where only the dominant scaling is exhibited. Then, by Eq. (24), *the failure time τ_f scales similarly to τ^*. We have thus derived analytic expressions for the failure time τ_f, the onset or precursor time τ^*, and the critical cluster size $\hat{c}$ that begins the avalanche. These are main results of this paper, and clearly demonstrate the size-scaling of the failure process deriving from the underlying rate law of Eq. (1).*

In the work of Phoenix and Tierney (PT), the time τ^* was postulated to be the failure time, in essence, and then PT used their asymptotic short-time results which are identical to our short-time results to obtain scalings for $\hat{c}$ and τ^* that are identical to the scalings obtained above.[11] The validity of taking τ^* as a good approximation to the failure time was supported by exact calculations on a system of size $N_T=10$ and $\eta=20$. Our results demonstrate that the failure time does scale like τ^* and that there is a fixed difference between τ^* and τ_f. For the case studied by PT, we predict the difference to be 10%, which is in good agreement with the difference exhibited in PT.[11] The range of applicability of the scalings found by PT was previously unknown, and PT expected their asymptotic results to break down below about $\eta=10$. The analysis here indicates that the scalings are actually appropriate down to the transition point $\eta>2$, with the recognition that the difference between τ^* and τ_f grows to be significant.

All of the scaling behavior is predicted to be algebraic in the logarithm of the system size. However, since the exponent $\eta/2-1$ can be large, the decrease in failure time can be very evident even over modest increases in system size. The appearance of the particular exponent $\eta/2-1$ explicitly demonstrates that the value of $\eta=2$ is the critical value for the transition to the avalanche regime for square-root stress concentrations. For $\eta=2$, there is no predicted size dependence and in fact τ^* is never attained.

The predicted critical crack size $\hat{c}$ initiating the avalanche grows only very slowly with system size, and decreases with increasing η. Thus, for larger η and moderate system sizes, the value of $\hat{c}$ is not large. Our neglect of cluster-cluster interactions and our limitation of the cluster shapes to a quasilinear form are supported by the fairly small values of $\hat{c}$ predicted by Eq. (25) (for $\eta=4$ and $N_T=10^6$, $\hat{c}\approx 11$ and for $N_T=10^8$, $\hat{c}\approx 13$ while for $\eta=8$ and $N_\tau=10^6$, $\hat{c}\approx 4$). In other words, large multiply branched clusters are not responsible for the onset of failure.[19]

B. Failure time distributions

Equations (24) and (26) prescribe the characteristic failure time τ_f, at which point the failure probability is 0.632 [see Eqs. (6) and (9)]. Of importance for reliability is the distribution of failure times around the characteristic time, and the size scaling of that distribution. We discuss approaches to obtaining this distribution below.

Since the characteristic failure time τ_f is determined by the formation of the critical $\hat{c}$ cluster at τ^*, we postulate that the failure time distribution is controlled by the probability of appearance of the size $\hat{c}$ crack vs time. The $\hat{c}$ cluster may appear earlier than, or later than, the typical time τ^*, but once formed we postulate that it grows to failure in the fixed time $\tau_f - \tau^*$. The cumulative probability of forming a size $\hat{c}$ cluster versus time is, from Eq. (6),

$$P(\hat{c},\tau) = 1 - \exp(-N_T R(\hat{c},\tau)), \tag{27}$$

and at time τ^* the probability is 0.632. The corresponding probability of complete failure (probability of finding a crack of size $c=L$ versus time τ) is then obtained by a *rigid shift* of this cumulative probability forward in time by the amount $\tau_f - \tau^*$:

$$P(L,\tau) = P\left(\hat{c}, \tau - \frac{2}{\eta}\,\tau_f\right), \tag{28}$$

where τ_f refers to the typical failure time in a system of linear size L so that $P(L,\tau_f)=0.632$. The failure time distribution determined from the full numerical results of Eq. (13) is shown in Figs. 5(a) and 5(b) along with the values obtained by a rigid shift of Eq. (28), and the agreement is quite good. Over the middle range of the probability distribution, the failure is controlled by the appearance of the $\hat{c}$ cluster. At lower probabilities, there is some deviation and the predicted probability of failure is not conservative, which drives us to consider improved descriptions shortly.

Using the short-time solution $R(\hat{c},\tau)\approx N(\hat{c},\tau)\propto\tau^{\hat{c}}$, the failure probability from Eqs. (27) and (28) is Weibull in form with the critical size $\hat{c}$ as the Weibull modulus:

$$P(\hat{c},\tau) = 1 - e^{-(\tau/\tau^*)^{\hat{c}}} \tag{29a}$$

and

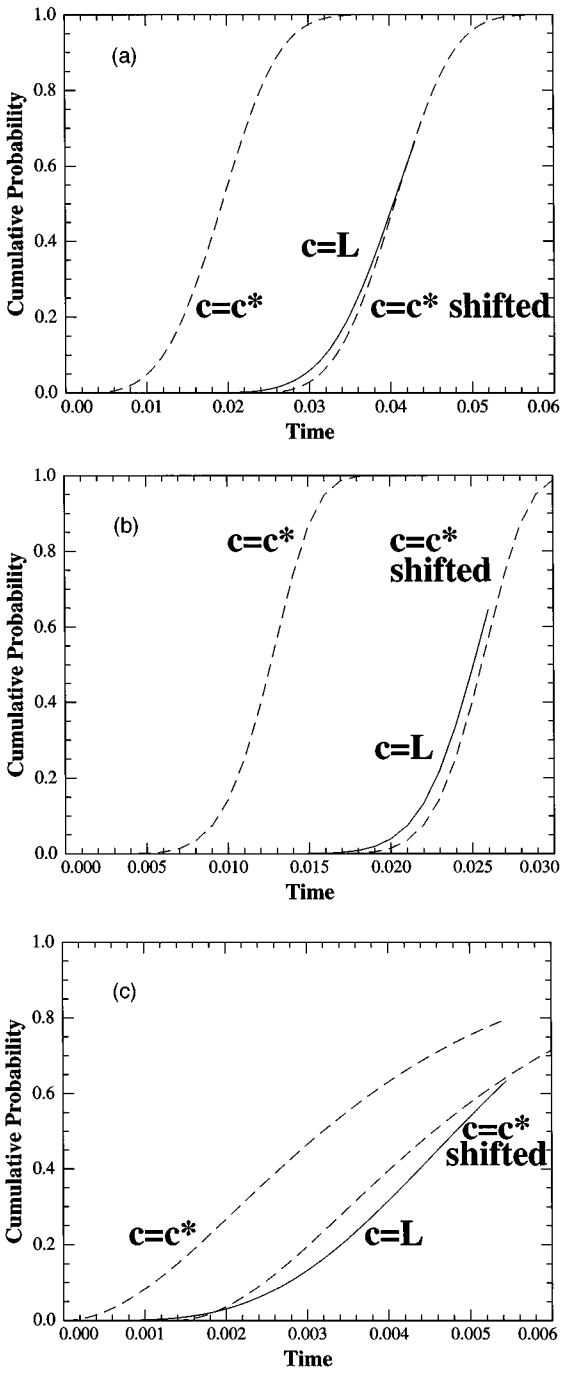

FIG. 5. Probability of failure versus time. The solid line is the full numerical result; short dashed line is the probability of obtaining cluster of size $\hat{c}$ versus time; long-dashed line is the probability of size $\hat{c}$ rigidly shifted by $2\tau_f/\eta$. (a) $\eta=4$, $N_T=10^4$; (b) $\eta=4$, $N_T=10^6$; (c) $\eta=8$, $N_T=10^4$.

$$P(L,\tau)=1-\exp\left[-\left(\frac{\tau-(2/\eta)\tau_f}{(1-2/\eta)\tau_f}\right)^{\hat{c}}\right]^{1/2}. \tag{29b}$$

Phoenix and Tierney also predicted the above Weibull distributions based on the asymptotic/short-time limit.[11] Tierney further improved the analysis to obtain better Weibull distributions for the low-probability tail.[12,13] For a Weibull distribution of modulus $\hat{c}$, the coefficient of variation (c.o.v. =standard deviation divided by the mean) is closely approximated by $1.2/\hat{c}$. From Eqs. (29a) and (29b) we see that the mean is shifted by a constant factor while $\hat{c}$ stays the same, and hence the c.o.v. for the failure time distribution is

$$\text{c.o.v.}\sim\frac{1}{\hat{c}}\sim\frac{\eta/2-1}{\ln N_T}, \tag{30}$$

where only the dominant scaling is shown. The c.o.v. decreases weakly with size N_T, and in a manner that is *independent* of η. At fixed size, the c.o.v. increases with increasing η because the material is much more sensitive to fluctuations in the damage at larger η. *Hence, at higher* η *the failure simultaneously becomes more abrupt* ($\tau^*\to\tau_f$) *and less predictable.*

Further refinements in estimating the failure time distribution are subtle. Weak-link scaling concepts are not strictly applicable here: failure in a subvolume of material does not immediately cause failure in the entire volume because the crack spanning the subvolume must still grow across the remaining cross section to fail the entire volume. A relationship between failure distributions of different size systems can be derived, however, which leads to a new more accurate form for the probability distribution. First, note that the failure probability of Eq. (6) involves N_T and $R(c,t)$. From the differential equations for $N(c,t)$ and the definition of $R(c,t)$, we also see that $R(c,t)$ does not involve the system size explicitly or implicitly. Hence, we can uniquely relate the probability distributions of different size systems through their common $R(c,t)$.

Let the probability of finding a crack of size c in volume N_i be $P_i(c,\tau)$. The probability of failure of a size N_1 system is then $P_1(L_1,\tau)$ where $L_1=N_1^{1/2}$, as usual. Solving Eq. (6) with $c=L_1$ for $R(L_1,\tau)$ in terms of $P_1(L_1,\tau)$, and then using this $R(L_1,\tau)$ in Eq. (6) for a system size of N_2, we obtain the probability distribution for the occurrence of an L_1 crack anywhere in a volume N_2 as

$$P_2(L_1,\tau)=1-[1-P_1(L_1,\tau)]^{N_2/N_1}. \tag{31}$$

This result is an upper bound to the actual failure distribution for size N_2, i.e., $P_2(L_2,\tau)\leqslant P_2(L_1,\tau)$.

Now, if L_1 is larger than the critical size $\hat{c}_2$ required for rapid growth of the dominant crack in the N_2 volume, then the L_1 cluster will grow to size L_2 precisely following the large-cluster growth of Eq. (21). The time to fail the size N_2 system is thus a time $\Delta\tau_{1\to2}$ longer than the time τ to form the L_1 cluster, where

$$\Delta\tau_{1\to2}=\int_{L_1}^{L_2}\frac{dc^*}{\alpha_c^*}=\frac{1}{z(1+1/z)^{\eta}(\eta/2-1)}\times\left[\frac{1}{L_1^{\eta/2-1}}-\frac{1}{L_2^{\eta/2-1}}\right]. \tag{32}$$

The failure probability of size N_2 then satisfies

$$P_2(L_2,\tau)=P_2(L_1,\tau-\Delta\tau_{1\to2})=1-[1-P_1(L_1,\tau-\Delta\tau_{1\to2})]^{N_2/N_1}, \tag{33}$$

which exactly relates the failure distribution of size N_2 to that of the smaller size N_1.

The relation Eq. (33) can now be used to find the failure distribution $P_1(L_1,\tau)$ from the characteristic failure times

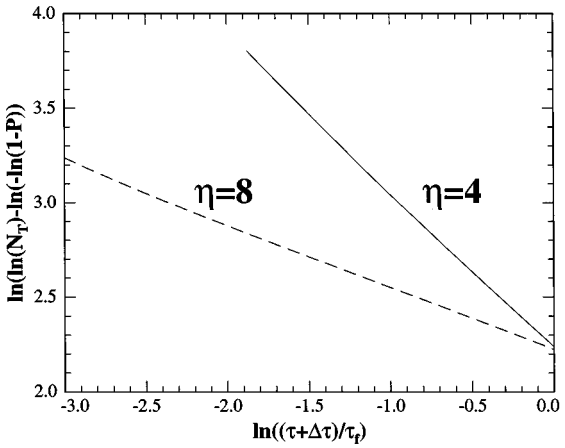

FIG. 6. Scaling of failure probability P vs time τ ($N_T=10^4$ and $\eta=4,8$) as calculated from Eq. (14), which from Eq. (39) should be linear if plotted as $\ln[\ln N_T-\ln(\ln(1-P))]$ vs $[(\tau+\Delta\tau)/\tau_f]$. The predicted slope is $(1-\eta/2)^{-1}$, which is close to the calculated value in each case.

for larger systems, which are accurately known from Eqs. (24)–(26). Specifically, suppose we know the characteristic failure time τ_2 for size N_2, i.e.,

$$P_2(L_2,\tau_2)=0.632, \tag{34}$$

for all system sizes $N_2>N_1$. Inverting Eq. (33) at time τ_2 then gives the failure probability for size N_1 at time $\tau_2-\Delta\tau_{1\to2}$ as

$$P_1(L_1,\tau_2-\Delta\tau_{1\to2})=1-0.368^{N_1/N_2}. \tag{35}$$

So, given a time τ at which we want $P_1(L_1,\tau)$, we first find the size N_2 such that $\tau=\tau_2-\Delta\tau_{1\to2}$ and then use this N_2 on the rhs of Eq. (35) to obtain the probability. For small probabilities/large N_2 we can carry this through analytically because for $N_2\gg N_1$ the time shift $\Delta\tau_{1\to2}$ becomes independent of N_2. Using the scaling of Eq. (26) for the failure time τ_2 we thus have

$$\tau=\tau_2-\Delta\tau_{1\to2}=D(\ln N_2)^{1-\eta/2}-\Delta\tau_{1\to2}, \tag{36}$$

and solving for N_2 yields

$$N_2=\exp\left[\left(\frac{\tau+\Delta\tau_{1\to2}}{D}\right)^{1/(1-\eta/2)}\right] \tag{37}$$

where D is some constant. Substituting Eq. (37) into Eq. (35) then yields

$$P_1(L_1,\tau)=1-\exp\left[-N_1\exp\left(-\left(\frac{\tau+\Delta\tau_{1\to2}}{D}\right)^{1/(1-\eta/2)}\right)\right]. \tag{38}$$

The failure probability is thus of the *double-exponential form* with an additional shift $\Delta\tau_{1\to2}$ dependent on the size N_1. This result is valid for short times (i.e., somewhat smaller than the characteristic failure time for size N_1) corresponding to large N_2, $N_2\gg N_1$, but with the weak restriction that $\hat{c}_2<L_1$. The only real approximations used in obtaining Eq. (38) is the scaling relation of Eq. (26) and the approximate N_2 independence of the time shift in Eq. (31). In Fig. 6 is shown a test of the scaling predicted by Eq. (38). Specifically, we have plotted $\ln[\ln N_1-\ln(-\ln(1-P))]$ vs $\ln[(\tau+\Delta\tau_{1\to2})/\tau_f]$ for $N_1=10^4$ and $\eta=4,8$. According to Eq. (38), the plot should then be a straight line of slope $(1-\eta/2)^{-1}$; the data in Fig. 6, where P is obtained from Eq. (13) and $\Delta\tau_{1-2}$ from Eq. (32), is nearly linear and essentially confirms the predicted double-exponential scaling over a wide range of probability. The slope for $\eta=4$ is slightly lower than the predicted value of -1, but is still nearly linear. Equation (38) is a great improvement over the simple Weibull ansatz of Eqs. (27)–(29) in the low-probability tail, although the simple Weibull captures the essence of the probability distribution. The double-exponential form has been shown to be the appropriate distribution function for static failure problems, but it is also accepted that distinguishing between a Weibull form and a double-exponential can be difficult unless a very broad range of sizes or stresses (here, times) are investigated.[20]

V. DISCUSSION

We have discussed a model to capture what we believe is the essence of the complex time-dependent failure driven by nucleated damage. We have found subtle relationships between the macroscopically measured failure time, failure time distribution, critical cluster size, and the underlying nonlinear driving factor η and system size. The details of the predicted scalings will be fully compared to numerical simulations in the companion paper, but the trends in behavior are very consistent with previous simulation results.

The present damage model and analysis also predict a failure probability consistent with the empirical Coleman model.[4] The Coleman model describes the failure probability versus time and applied stress σ as

$$P(\sigma,t)=1-\exp\left\{-\left[\int_0^t\frac{dt'}{t_0}\left(\frac{\sigma}{\sigma_0}\right)^{\beta}\right]^{\rho^*}\right\}, \tag{39}$$

where t_0, σ_0, β, and ρ^* are parameters. Under constant stress this simplifies to

$$P(\sigma,t)=1-\exp\left\{-\left(\frac{\sigma}{\sigma_0}\right)^{\beta\rho^*}\left(\frac{t}{t_0}\right)^{\rho^*}\right\}. \tag{40}$$

The present results for the onset of failure around τ^* can be written in dimensional form following from Eq. (29a) as

$$P(t)=1-\exp\left\{-\left(\frac{t}{t^*}\right)^{\hat{c}}\right\}. \tag{41}$$

But since t^* implicitly depends on applied stress we can write more generally

$$P(\sigma,t)=1-\exp\left\{-\left(\frac{\sigma}{\sigma_0}\right)^{\eta\hat{c}}\left(\frac{t}{t_0^*}\right)^{\hat{c}}\right\}, \tag{42}$$

where t_0^* is the onset time at some reference stress σ_0. The final failure probability of Eq. (29b) adopts a similar form. A comparison of Eqs. (40) and (42) shows them to be identical with the association of $\rho^*=\hat{c}$ and $\beta=\eta$. If the applied stress changes with time, the effect on the present model is to speed up or slow down the damage evolution proportionally but the progression of damage does not otherwise change, as

shown in the Appendix. Hence, the present results are also consistent with the full Coleman model of Eq. (39). In contrast to the Coleman model, however, the present model has underlying damage-rate parameters A and η which then lead to predicted (size-dependent) quantities t_0^* and $\hat{c}$ at some applied stress σ_0.

The present model is also consistent with the linear Monkman-Grant relationship.[5] Specifically, the minimum creep rate in the present model is $\dot{\varepsilon}$ at short times, where only isolated clusters are formed. So, with $\varepsilon \sim 1/E(t) \sim 1 + (\beta/N_T)\Sigma_c c^2 N(c,t)$ we have $\dot{\varepsilon}_{\min} \sim dN(1,t)/dt$ at short times and hence $\dot{\varepsilon}_{\min} \sim \alpha_0 = 1/A\sigma_{\text{app}}^{\eta}$. The failure time is $t_f = \tau_f A \sigma_{\text{app}}^{\eta}$ where τ_f is a pure dimensionless number. Thus,

$$\dot{\varepsilon}_{\min} t_f = \tau_f , \tag{43}$$

which is the Monkman-Grant relationship between creep rate and failure time.

A major conceptual approximation in the present work is the neglect of linking of smaller clusters to form larger clusters. Such linking could cause the formation of a critical crack at much earlier times than predicted here, and modify the scalings. We have previously considered linking in the case of a one-dimensional system ($z=2$) where two clusters of sizes c,c' separated by a single intervening site are allowed to link by a stress concentration $\sigma_{c,c'}$ which may be quite enhanced relative to the isolated crack stress concentrations. Here, we consider only the short-time limit with linking and show that the time dependence for formation of a size c crack still scales with τ^c. Specifically, considering Eqs. (A1)–(A6) in Ref. 18 and considering the limit of small numbers of clusters (short times) leads to the differential equations

$$\frac{dN(c,\tau)}{d\tau} = \alpha_{c-1} N(c-1,\tau) + \frac{1}{2}\sum_{c'=1}^{c-2} \alpha_{c-c'-1,c'} N(c',\tau) \times N(c-c'-1,\tau) \quad c \geqslant 3, \tag{44}$$

where $\alpha_{c-c'-1,c'} = \sigma_{c-c'-1,c'}^{\eta}$ is the linking rate for clusters of sizes $c-c'-1$ and c'. The first term on the rhs of Eq. (44) is the simple single-step growth term while the second term is due to all of the possible linking steps that can form a size c cluster. The solution to Eq. (44) is of the form $N(c,\tau) = f_c \tau^c$ where the coefficient f_c satisfies the recursion relation

$$f_c = \frac{1}{c}\left(\alpha_{c-1} f_{c-1} + \sum_{c'=1}^{c-2} \alpha_{c-c'-1,c'} f_{c-c'-1} f_{c'} \right) \quad c \geqslant 3. \tag{45}$$

The effect of the linking changes the prefactor of the power law but not the form of the scaling.

In the most extreme case, one-half of the stress carried by the two clusters could be shed onto the one intervening site so that

$$\alpha_{c-c'-1,c'} = \left(\frac{c-1}{2} \right)^{\eta}. \tag{46}$$

Numerical evaluation of the coefficients f_c then shows the following behavior for various η. For $\eta=0$, the coefficients become much larger and the exact $1-d$ percolation solution is regained, as shown in Ref. 18. For $\eta=2$, the coefficients are slightly larger by a factor of approximately $1+0.03c$, which has almost no effect on the overall scaling behavior or the location of the transition to avalanche behavior. For $\eta=4$, the coefficients are larger by 2–3 % independent of c, while for $\eta=8$ the coefficients are larger by only 0.1%, again independent of c. The modifications to the coefficients thus have negligible effects on the overall scaling behavior of the failure. Some details of the precise evolution such as actual failure time and the time τ^* will be changed very slightly in magnitude, but the scalings predicted in this paper are expected to be quite accurate. These results are consistent with the analysis of Phoenix and Tierney, who also derived the recursion relation of Eq. (45) by a different approach.

As mentioned earlier, the problem of damage evolution studied here has been previously considered in detail by Phoenix and Tierney (PT),[11] Tierney,[12,13] and Kuo and Phoenix[14] for the one-dimensional case of linear clusters ($z=2$). PT provided exact recursions relations for the failure time distributions of increasing system sizes but the recursions were not easily extendable to large systems. They thus performed asymptotic analyses for large η and short times, and obtained results for $R(c,\tau)$ and $P(c,\tau)$ analogous to our short-time results of Eq. (14) and showed that the linking processes can be neglected at early times, as suggested also by our Eq. (45). These workers then demonstrated that the envelope formed by the absolute lower bounds of the entire family of $P(c,\tau)$ $c=1,2,3\ldots$ formed an apparently rapidly convergent function $1-\exp(-\hat{W}(t))$ for the failure probability, with each $P(c,\tau)$ a Weibull function. The accuracy of the function $\hat{W}(t)$ was validated by comparison to an exact calculation of the true $W(t)$ on a system of size $N_T=10$ and $\eta=20$, as noted earlier. This agreement led PT and others to propose $\hat{W}(t)$ as an accurate estimate to the true failure distribution, and to use the short-time/asymptotic results to derive scalings for the key quantities τ^* and $\hat{c}$. PT anticipated a possible breakdown in these scalings for smaller η, but our results suggest otherwise. We have proceeded differently but have obtained many similar results by using the short-time limits as well. The important differences with the work of PT are (i) we have considered small η and shown a transition to percolationlike behavior, (ii) we have demonstrated a special relationship between the true failure time and the time τ^* so that the scaling of τ^* is appropriate to failure, (iii) we have demonstrated the applicability of the asymptotic results to essentially all $\eta>2$, and (iv) we have proposed a different analytic form for the $W(t)$ function [Eq. (38)]. Our results, where different than PT, are thus very complementary to that extensive work.

We have also recently uncovered a short paper in the Russian literature by Gotlib *et al.* which addresses the general problem discussed here.[21] ''Kinetic equations'' similar to Eq. (13) were derived for the evolution of the cluster distribution, and the short-time solution was explicitly presented. In addition, these authors proposed a condition under which the short-time solution becomes invalid, and postulated that the largest cluster at this time would then grow sequentially across the specimen to failure. The condition for crossover from the short-time regime to a growth regime is identical to the condition Phoenix and Tierney used for failure, but Gotlib *et al.* also recognized the key presence of an additional time increment for growth to failure. Conceptu-

ally, the ideas of Gotlib *et al.* are thus very similar to those put forth here and in our earlier work. Here, however, we demonstrate explicitly the transition in failure behavior versus the nonlinearity η, and also how the onset of unstable (avalanche) growth begins around a characteristic time τ^*. We then use the short-time approximation for the cluster size distribution, but only to obtain the size scalings. Our results for the probability distribution of the failure time were also unanticipated in the work of Gotlib *et al.*

The model discussed here is a time-dependent analog to the static fracture models developed to describe failure in systems with heterogeneously distributed static fracture strengths.[22] Both types of models neglect long-range interactions and focus only on the growth of existing clusters, or the formation of new clusters. In the time-dependent problem studied here the heterogeneity is self-generated by the evolution of the damage itself, and there is no heterogeneity in the local failure rates. Furthermore, failure in the present problem is not instantaneous but rather stems from the onset of an accelerating growth process. This latter aspect makes the present problem somewhat more tractable than the time-independent problems, where there is an actual fracture threshold.

A particularly important result of the present work is the identification of a precursor onset time τ^* that presages failure. The macroscopic conditions (strain, strain rate, etc.) prevailing around τ^* will be the subject of further investigation to determine if the onset of avalanche failure can be identified macroscopically. Such an identification may be difficult, but represents a critical step toward understanding reliability and failure avoidance in real materials.

In a companion paper we perform extensive numerical simulations on the present damage problem, and compare the results of those simulations to the analytic model predictions discussed here. The overall results show that, with a modification to the stress concentration factors to match those of the discrete model used in the simulations, one obtains quantitative agreement between theory and ''experiment'' for absolute failure times, general nature of the failure mode, and scaling of the failure times. This detailed comparison supports the approximations made in the analytic model and provides confidence that similar concepts can be applied to more complex and heterogeneous time-dependent failure processes.

ACKNOWLEDGMENTS

The authors thank the National Science Foundation, Division of Materials Research, Materials Theory, for support of this work through Grant No. DMR-9420831, and Professor S. L. Phoenix for a critical reading of the manuscript and constructive comments on the work.

APPENDIX: INCLUSION OF AVERAGE CLUSTER INTERACTIONS

Since the rates of damage formation depend sensitively on the local stresses, interactions which increase the local stresses will, at the very least, accelerate the damage process. Here, we discuss how to account for cluster interactions in an average, or mean-field manner. Note that as the damage accumulates, the elastic modulus $E(\tau)$ decreases [Eq. (3)]. This modulus decrease is a reflection of the average *increasing* stress born by the remaining undamaged sites, even though the externally applied stress is fixed at $\sigma_{\rm app}$. To fold back this average increasing stress into the damage accumulation process, one can envision that there is an *effective* externally applied stress $\sigma_{\rm app}^{\rm eff}(\tau)$ acting on the entire system at time τ. This effective stress, reflecting *average* cluster interactions, is simply

$$\sigma_{\rm app}^{\rm eff}(\tau)=\sigma_{\rm app}E(0)/E(\tau). \tag{A1}$$

Since this effective stress is applied to all undamaged sites equally, *it does not effect the distribution of damage*, only the time required to attain any prescribed level of damage is affected. Since $\sigma_{\rm app}^{\rm eff}(\tau)\geqslant\sigma_{\rm app}$, the rate of damage accumulation is accelerated by including interactions. To demonstrate this formally, we rewrite Eq. (11) by replacing $\sigma_{\rm app}$ by $\sigma_{\rm app}^{\rm eff}(\tau)$. Defining a new time increment $d\tilde{\tau}$ as

$$d\tilde{\tau}=\left[\frac{\sigma_{\rm app}^{\rm eff}(\tau)}{\sigma_{\rm app}}\right]^{\eta}d\tau, \tag{A2}$$

we can rewrite Eq. (13) in terms of the new time variable $\tilde{\tau}$ as

$$\frac{dN(c,\tilde{\tau})}{d\tilde{\tau}}=\alpha_{c-1}N(c-1,\tilde{\tau})-\alpha_cN(c-1,\tilde{\tau}), \tag{A3}$$

which is identical to Eq. (13) with τ replaced by $\tilde{\tau}$. Thus the cluster distribution $N(c,\tau)$ obtained at time τ without average interactions is attained at an earlier time $\tilde{\tau}$ in the presence of interactions:

$$N(c,\tau)_{\rm no\ interactions}=N(c,\tilde{\tau})_{\rm interactions} \tag{A4}$$

with

$$\tilde{\tau}=\int_0^{\tau}d\tau'\left[\frac{\sigma_{\rm app}}{\sigma_{\rm app}^{\rm eff}(\tau'')}\right]\leqslant\tau. \tag{A5}$$

In terms of the examples for c shown in Fig. 4, only the times indicated in the figures are modified by including the average interactions.

[1] *Methods for Assessing Structural Reliability of Brittle Materials, ASTM 844*, edited by S. W. Freiman and C. M. Hudson (American Society for Testing Materials, Philadelphia, 1984); B. Lawin, *Fracture of Brittle Solids* (Cambridge University Press, Cambridge, England, 1993).

[2] J. R. Brockengrough, S. Suresh, and J. Duffy, Philos. Mag. A **58**, 619 (1988); S. Suresh and J. R. Brockenbrough, Acta Metall. Mater. **38**, 55 (1990).

[3] J. R. Porter, W. Blumenthal, and A. G. Evans, Acta Metall. **29**, 1899 (1981); B. J. Dalgleish, E. B. Slamovich, and A. G. Evans, J. Am. Ceram. Soc. **68**, 575 (1985); W. Blumenthal and A. G. Evans, *ibid.* **67**, 751 (1984); H. C. Cao, B. J. Dalgleish, C.-H.

Hsueh, and A. G. Evans, *ibid*. **70**, 257 (1987).
[4] B. D. Coleman, J. Appl. Phys. **28**, 1058 (1957); Trans. Soc. Rheol. **28**, 195 (1958); J. Appl. Phys. **29**, 968 (1958); B. D. Coleman and A. G. Knox, Text. Res. J. **27**, 393 (1957).
[5] F. C. Monkman and N. J. Grant, Proc. ASTM **56**, 593 (1956).
[6] S. M. Wiederhorn, B. J. Hockey, and T. J. Chuang, in *Toughening Mechanisms in Quasi-Brittle Materials*, edited by S. P. Shah (Kluwer, Dordrecht, 1991), p. 555; S. M. Wiederhorn, D. E. Roberts, and T. J. Chuang, J. Am. Ceram. Soc. **71**, 602 (1988).
[7] S. M. Wiederhorn and B. J. Hockey, in *Advanced Structural Inorganic Composites, 7th CIMTEC-World Ceramics Congress*, edited by P. Vincenzini (Elsevier, Amsterdam, 1991), p. 365; B. A. Fields and S. M. Wiederhorn, J. Am. Ceram. Soc. **79**, 977 (1996).
[8] D. F. Carroll and R. E. Tressler, J. Am. Ceram. Soc. **68**, 143 (1985); **71**, 472 (1988); **72**, 49 (1989).
[9] W. A. Curtin and H. Scher, Phys. Rev. Lett. **67**, 2457 (1991).
[10] A. Hansen, S. Roux, and E. L. Hinrichsen, Europhys. Lett. **13**, 517 (1990).
[11] S. L. Phoenix and L. J. Tierney, Eng. Fract. Mech. **18**, 193 (1983).
[12] L. Tierney, Adv. Appl. Probab. **14**, 95 (1982).
[13] L. Tierney, Stochast. Proc. Appl. **18**, 139 (1984).
[14] C.-C. Kuo and S. L. Phoenix, J. Appl. Probab. **24**, 137 (1987).
[15] B. Budiansky and R. J. O'Connel, Int. J. Solids Struct. **12**, 81 (1976).
[16] N. Laws and J. R. Brockenbrough, Int. J. Solids Struct. **23**, 1247 (1987).
[17] R. Raj, J. Am. Ceram. Soc. **15**, C-46 (1982).
[18] W. A. Curtin and H. Scher, Phys. Rev. B **45**, 2620 (1992).
[19] W. A. Curtin and H. Scher, Phys. Rev. Lett. **70**, 101 (1992); S. Roux, A. Hansen, and E. L. Hinrichsen, *ibid*. **70**, 100 (1992).
[20] P. M. Duxbury, P. D. Beale, and P. L. Leath, Phys. Rev. Lett. **57**, 1052 (1986); P. M. Duxbury, P. L. Leath, and P. D. Beale, Phys. Rev. B **36**, 367 (1987); P. M. Duxbury and P. L. Leath, *ibid*. **49**, 12 676 (1994).
[21] Y. Y. Gotlib, A. V. Dobrodumov, A. M. Elyashevich, and Y. E. Svetlov, Sov. Phys. Solid State **15**, 555 (1973).
[22] P. M. Duxbury and P. L. Leath, Phys. Rev. Lett. **72**, 2805 (1994); D. G. Harlow and S. L. Phoenix, Int. J. Fract. **17**, 601 (1981); P. L. Leath and P. M. Duxbury, Phys. Rev. B **49**, 14 905 (1994).